JOINT INSTITUTE FOR NUCLEAR RESEARCH
Frank Laboratory of Neutron Physics

FINAL REPORT ON THE START PROGRAMME

Structure of calixarenes containing eight-arm poly-2-alkyl-2-oxazoline arms with polymethacrylic acid

Supervisor:
PhD Yulia E. Gorshkova

Student:
Mityushkin Evgeniy,
Kazan Federal University

Participation period:
July 16 – August 13,
September 2 – October 15
Summer Session 2022

Dubna, 2022

Abstract

In this work, the structure of the synthesis of new starlike eight-arm poly-2-alkyl-2-oxazolines with specific calixarene branches is calculated and maintained by the order of connection of the polyoxazoline arms to the calixarene macrocycle. Measurement was done by small-angle neutron scattering and atomic force microscopy.

Introduction

During the summer student practice at the Frank Laboratory of Neutron Physic of Joint Institute for Nuclear Research (JINR) according to the START program, an analysis was made of starlike eight-armed poly-2-alkyl-2-oxazolines with a calixarene branching center and a different order of attachment of polyoxazoline arms to the calixarene macrocycle (Fig. 1). Two structural formulas of calixarenes based on sulfonyl chloride-type calixarene initiators were studied. For the synthesis of polymers of structure **I**, a polyfunctional initiator with sulfonyl chloride initiating groups introduced into the upper rim of the calixarene macrocycle was used. In contrast, the structure **II** polymer was obtained from a polyfunctional initiator with sulfonyl chloride initiating groups introduced into the lower rim of the calixarene macrocycle.

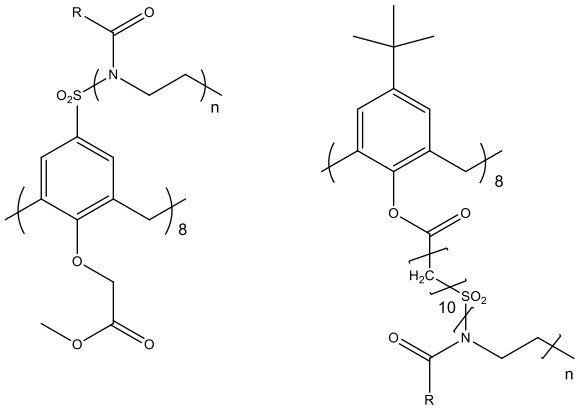

I **II**

Fig. 1 – Synthesis scheme for calixarenes

Starlike eight-armed poly-2-alkyl-2-oxazolines of structure **I** and **II** were obtained by cationic polymerization of 2-ethyl- and 2-isopropyl-2-oxazolines, excluding the cycle based on the synthesized initiators. Sulfolane is used as a solvent for cationic polymerization.

Initiator	Monomer	Name
I	2-ethyl-2-oxazoline	C1
	2-isopropyl-2-oxazoline	C2
II	2-ethyl-2-oxazoline	C3
	2-isopropyl-2-oxazoline	C4

Table 1 – Name of 4 calixarene complexes

During the summer practice at JINR, it was necessary to solve the following problem: to study the structure of the synthesized calixarenes. For the study, complementary methods were used: small-angle neutron scattering and atomic force microscopy.

Methods

SANS. Small-angle neutron scattering (SANS) is the elastic scattering of thermal neutrons by inhomogeneities of matter. Scattered neutrons deviate slightly from the direction of the incident beam: from 0.3 to 5 degrees. With their help, inhomogeneities of matter with a characteristic size of ~10-10^4 Å are explored. SANS is used to study the structure of biological molecules in solution, bulk defects in crystalline substances, the cluster structure of liquids and amorphous bodies, pores in various porous materials, etc. [1].

Let us consider the scattering of neutrons by the inhomogeneities of the matter with length size D. The main fraction of scattered radiation is concentrated in the region of scattering vectors:

$$q = |\vec{q}| = \frac{4\pi\sin\theta}{\lambda} \leq \frac{2\pi}{D},$$

where $\vec{q} = \vec{k} - \vec{k}_0$ – scattering vector; $\vec{k} = \frac{2\pi}{\lambda}\vec{q}$; θ - scattering angle; λ - wavelength.

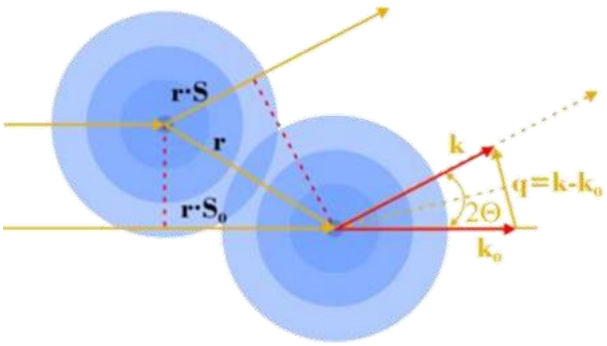

Fig. 2 – Scattering from atoms [2]

The scattering amplitude or form factor F(q) of an isolated molecule with N atoms can be determined Fourier Transform of the atomic distribution:

$$F(q) = \sum_{i=1}^{N} f_i(q)\exp\,(i\vec{q}\overrightarrow{r_i})$$

The scattered intensity from the isolated molecule is then

$$I(q) = |F(q)F^*(q)| = \sum_{i=1}^{N}\sum_{j=1}^{N} f_i(q)j(q)\exp\,(i\vec{q}(\overrightarrow{r_i} - \overrightarrow{r_j}))$$

After average over all orientations: $\langle\exp\,(i\vec{q}(\overrightarrow{r_i} - \overrightarrow{r_j}))\rangle = \frac{\sin(\vec{q}\overrightarrow{r_{ij}})}{\vec{q}\overrightarrow{r_{ij}}}$ the scattered intensity equal:

$I(q) = \sum_{i=1}^{N}\sum_{j=1}^{N} f_i(q)j(q)\frac{\sin(\vec{q}\overrightarrow{r_{ij}})}{\vec{q}\overrightarrow{r_{ij}}}$ – Debye formula

Each atomic distance r_{ij} in the molecule adds a sinx/x like term to the scattering intensity:

- Small distance: low frequency in sinx/x and dominate signal at high q;
- Large distance: high frequencies in sinx/x and dominate the signal at low q.

$$I(q) = \langle F(q)F^*(q)\rangle = \langle FT[\rho(\vec{r})]FT[\rho(-\vec{r})]\rangle = \langle FT[\rho(\vec{r})\rho(-\vec{r})]\rangle$$

The measured scattering intensity is the spherically averaged Fourier transform of the auocorrelation of the electron density of the particle.

$\gamma(\vec{r}) = [\rho(\vec{r})\rho(-\vec{r})]$ – autocorrelation function

$$\gamma(\vec{r}) = [\rho(\vec{r})\rho(-\vec{r})] = \int \rho(\vec{r}+\vec{u})\,\rho(\vec{r})dV$$

$$\gamma(r) = \frac{1}{2\pi^2}\int_0^{\infty} I(q)\frac{sin(qr)}{qr}q^2dq$$

For a homogeneous particle $\rho(\vec{r}) = \rho$, when $\vec{r} \in$ V, and = 0, when $\notin$V. Characteristic Function $\gamma_0(r) = \gamma(r)/\gamma(0)$ with $\gamma(0) = \rho^2V$.

Pair distance distribution function:

$$p(r) = r^2\gamma(r) = \rho^2Vr^2\gamma(r)$$

The pair distance distribution function represents the histogram of distances between pairs of points within the particle. D_{max} is the maximum diameter in the particle.

$$p(r) = 4\pi \int_0^\infty I(q)qrsin(qr)dq$$

R_g^2 is the average electron density weighted squared distance of the scatters from the centre of the object:

$$R_g^2 = \frac{\int r^2\rho(r)dr}{\int \rho(r)dr}$$ – radius of Gyration

- Solid sphere radius R: $R_g^2 = \frac{3}{5}R^2$;
- Ellipse with semiaxes a and b: $R_g^2 = \frac{a^2+b^2}{4}$;
- Spherical shell with R>r: $R_g^2 = \frac{3}{5}\frac{R^5-r^5}{R^3+r^3}$;
- Thin rod length L: $R_g^2 = \frac{1}{12}L^2$;
- Thin disk radius R: $R_g^2 = \frac{1}{2}R^2$.

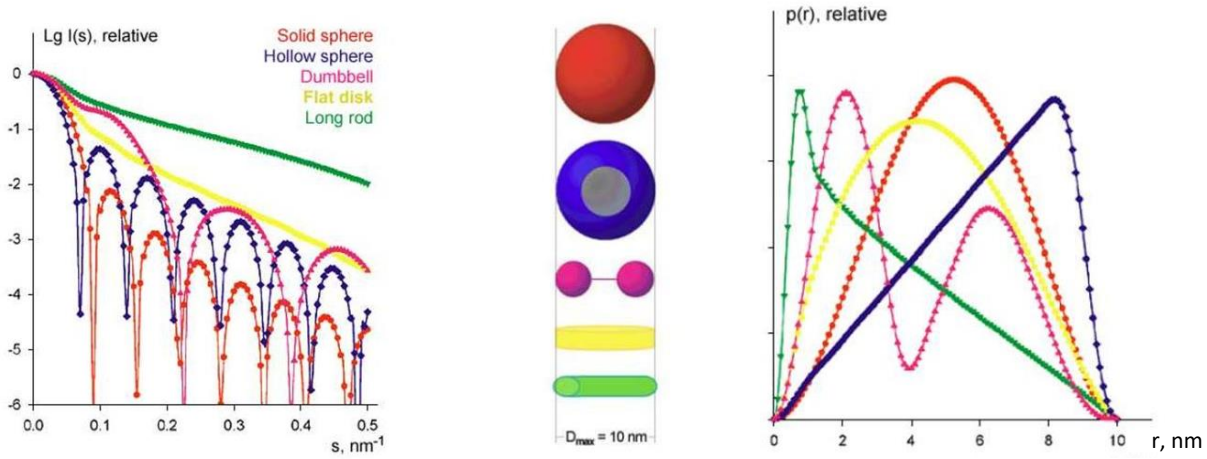

Fig. 3 – Scattering from model structures

The low q region of the scattering curve is characteristic for the overall dimension of the particle ($q \to 0$):

$I = I_0 exp(-1/3q^2R_g^2)$ – the Guinier approximation

Deviation from the straight line in the Guinier plot indicate intermolecular interaction or aggregation.

SANS equipment. For SANS measurement was used YuMO spectrometer (channel No. 4 at the IBR-2 reactor). For processing small angle scattering spectra SasView and Primus software were used.

Sample preparation for SANS. The solution of calixarene complexes was placed in quartz cuvettes, the inner thickness of which was 1 mm. Distilled water and distilled water + polymethacrylic acid were used as a buffer.

AFM. Atomic force microscopy (AFM) is a scanning probe microscopy that makes it possible to explore the microstructure and topographic features of a material with high resolution. AFM is based on measuring the force interaction between the surface of a sample and a microscope probe fixed at the end of an elastic cantilever. The force acting on the probe from the side of the sample causes the cantilever to bend. By registering the level of bending, it is possible to control the force of interaction between the probe and the surface. Interaction forces include Van-der-Waals force, adhesion and elasticity forces, magnetic and electrostatic forces. Depending on the nature of the acting force, several modes of AFM operation are distinguished: contact, non-contact and intermittent contact mode [3].

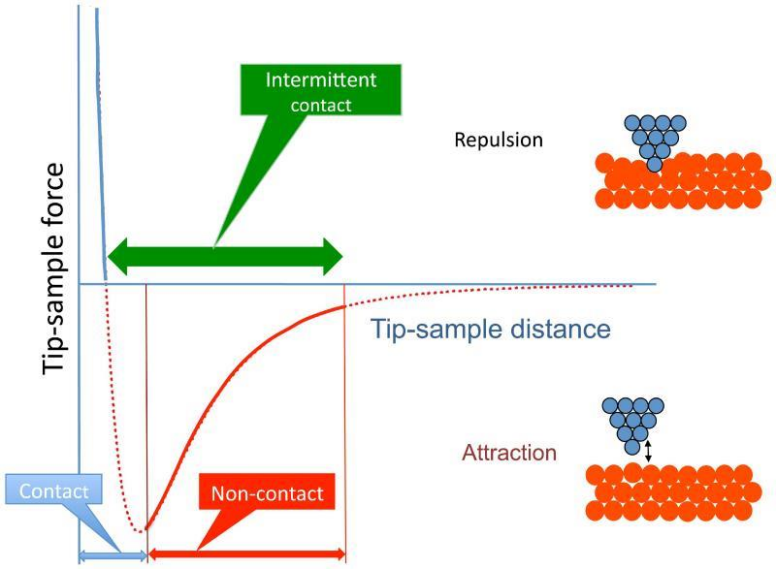

Fig. 4 – Dependence of Van-der-Waals force F of length z and modes AFM

The scheme of operation of an AFM is shown in fig. 5. The radiation of the semiconductor laser is focused on the cantilever. The reflected radiation is recorded using a photodiode consisting of four quadrants. The photodiode allows you to determine the direction and level of displacement of the cantilever arm.

Without load, laser radiation enters the center of the photodiode. The photocurrents taken from all sections of the photodetector are equal. During measurements, because of deformation of the console under the action of interaction forces, the reflected beam deviates from the initial position. This shift causes a change in the photocurrent for each section. A change in the photocurrent makes it possible to unambiguously characterize the level and direction of displacement of the cantilever arm. The photocurrent taken from the four sections of the photodetector generates a voltage in the feedback circuit (FC), which is recorded in the computer's memory as a surface relief.

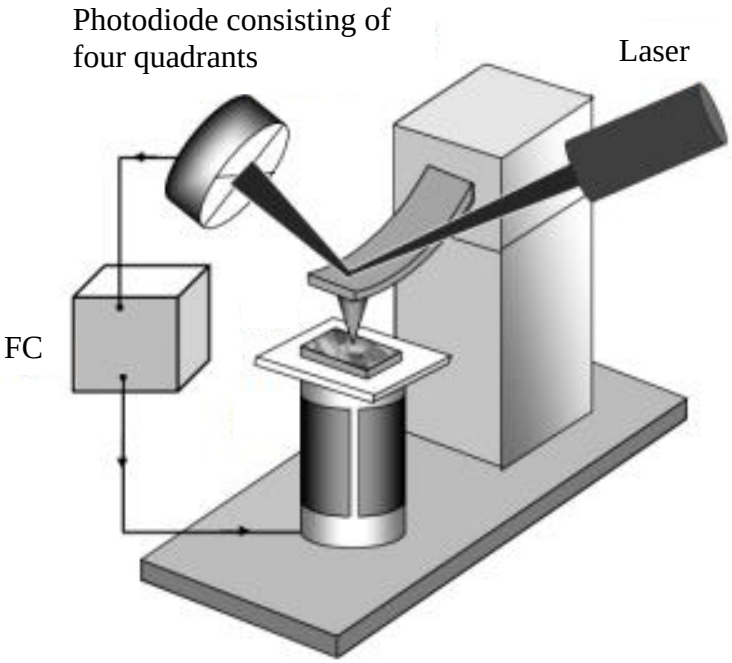

Fig. 5 - Scheme of operation of an atomic force microscope

In the contact mode, the distance between the probe and the surface is a few angstroms. This provides a balance between the forces of repulsion and attraction. Either scanning mode is used with a constant force of interaction between the probe and the sample, or with a constant average distance between the surface of the sample and the probe. In the first case, the level of cantilever bending is compensated by a feedback system, where the control voltage is proportional to the change in the surface topography. In the second, the image is a picture of the spatial distribution of the force acting on the probe from the surface.

The non-contact AFM mode is used to study biological objects and organic materials with low mechanical rigidity. The piezoelectric scanner excites cantilever oscillations with an amplitude of the order of hundreds of angstroms and a frequency of several hundred kilohertz. The presence of a force gradient acting on the probe from the surface leads to an additional shift of the resonant frequency. This causes a shift in the amplitude-frequency and phase-frequency characteristics to the region of low frequencies. Image construction in the non-contact mode is carried out by fixing local changes in the amplitude and phase of cantilever oscillations. The presence of an additional phase shift is used to obtain phase contrast.

In practice, the intermittent contact mode is more often used because of the versatility of this method. As in the non-contact mode, the piezo vibrator excites the cantilever at a frequency close to the resonant one. The distance between the probe and the sample corresponds to the touch in the lower half-cycle of the cantilever oscillations. The total interaction is determined by the elastic force at the moment of contact and the van der Waals forces. During scanning, the feedback system registers

local changes in the amplitude and phase of the cantilever oscillations, which form the image and the phase contrast distribution, respectively.

AFM equipment. In AFM experiments, NTEGRA PRIMA (NT-MDT Spectrum Instruments, Zelenograd, Russia) system was used. AFM images were recorded at intermittent contact mode, also known as tapping modeTM, with standard (NSG01_Au) tips of 10 nm curvature radius (NT-MDT Spectrum Instruments, Zelenograd, Russia) at room temperature. The imaging rate was 0.3 Hz.

Sample preparation for AFM. AFM image of the calixarene complexes surfaces obtained from solution of polymer in water with a concentration of 1:1000. The solution was applied to fresh prepared mica and kept for a minute. Then the mica was washed twice in distilled water and dried in air.

Experimental

For four types of calixarenes and their interpolymer complexes (IPCs) with polymethacrylic acid (PMA) (enhanced neutron scattering), small-angle neutron scattering was carried out (Fig. 6).

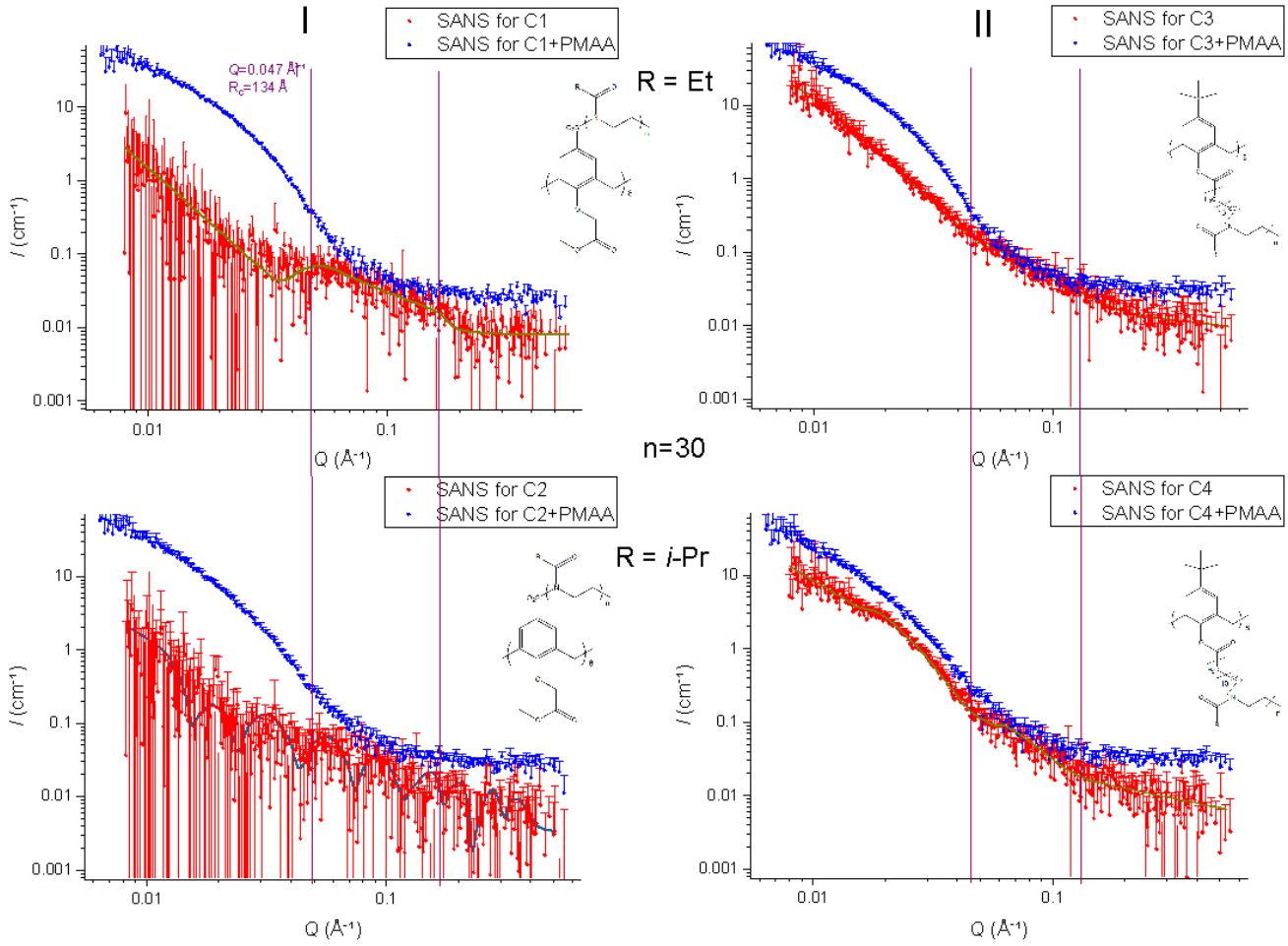

Fig. 6 – SANS carves for calixarene complexes C_1–C_4 and IPK carves with PMAA

To process the obtained small-angle scattering curves, we used the generalized empirical Guinier–Porod model:

The scattering intensity is determined by two contributions:

$$I(Q) = \frac{G}{Q^s}\exp\left(\frac{-Q^2R_g^2}{3-s}\right) \quad \text{for } Q \le Q_1,$$

$$I(Q) = \frac{D}{Q^d} \quad \text{for } Q \ge Q_1.$$

Q – scattering variable, $I(Q)$ – scattering intensity, R_g – gyration radius, d – Porod exponent, G и D – Guinier and Porod scale factors.

The s parameter is required for object modeling. For spherical objects s = 0, for rods s = 1, and for lamellas (or plates) s = 2. Dimension parameter is defined 3 - s.

From the continuity condition for the Guinier and Porod functions and their derivatives, with d > s and s < 3:

$$Q_1 = \frac{1}{R_g}\left[\frac{(d-s)(3-s)}{2}\right]^{1/2},$$

$$D = G\exp\left(\frac{-Q_1^2R_g^2}{3-s}\right)Q_1^{(d-s)}$$

$$= \frac{G}{R_g^{(d-s)}}\exp\left[-\frac{(d-s)}{2}\right]\left[\frac{(d-s)(3-s)}{2}\right]^{(d-s)/2}.$$

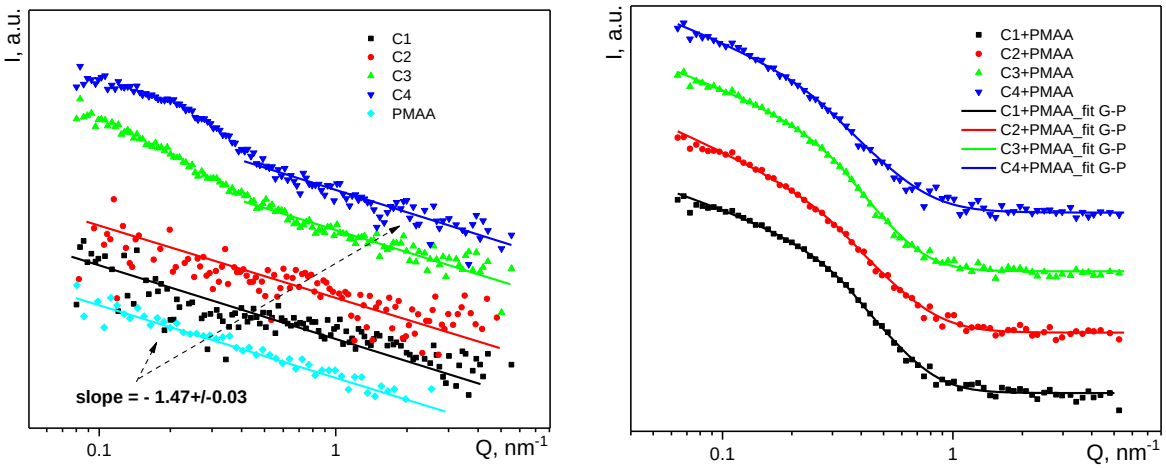

Fig. 7 – A) SANS carves of calixarene C_1-C_4 and PMAA; B) IPK calixarene with PMAA; Continues lines show the approximation according to the generalized Guinier-Porod model

IPK	R_g, Å	s	3 - s	d	Q_1
C_1 + PMAA	46,3 (1,7)	1,30 (0,06)	1,70	4,79 (0,09)	0,0372
C_2 + PMAA	37,2 (2,2)	1,71 (0,07)	1,29	4,20 (0,08)	0,0341
C_3 + PMAA	47,6 (2,0)	1,40 (0,07)	1,60	4,95 (0,10)	0,0354
C_4 + PMAA	44,3 (3,7)	1,53 (0,11)	1,47	4,01 (0,09)	0,0305

Table 2 – Parameters obtained from SANS curves analysis (SasView) of the general Guinier–Poroda model for IPK complexes calixarene C_1, C_2, C_3 and C_4 with PMAA

The size of the calixarene complexes was determined using the pair correlation function P(r). SasView and Primus software for processing small-angle scattering spectra were used. The obtained data were entered into the Table 3. To find the characteristic sizes R of molecules calixarene next observation [4]:

$$R = R_g \left(\frac{d+2}{d}\right)^{\frac{1}{2}}$$

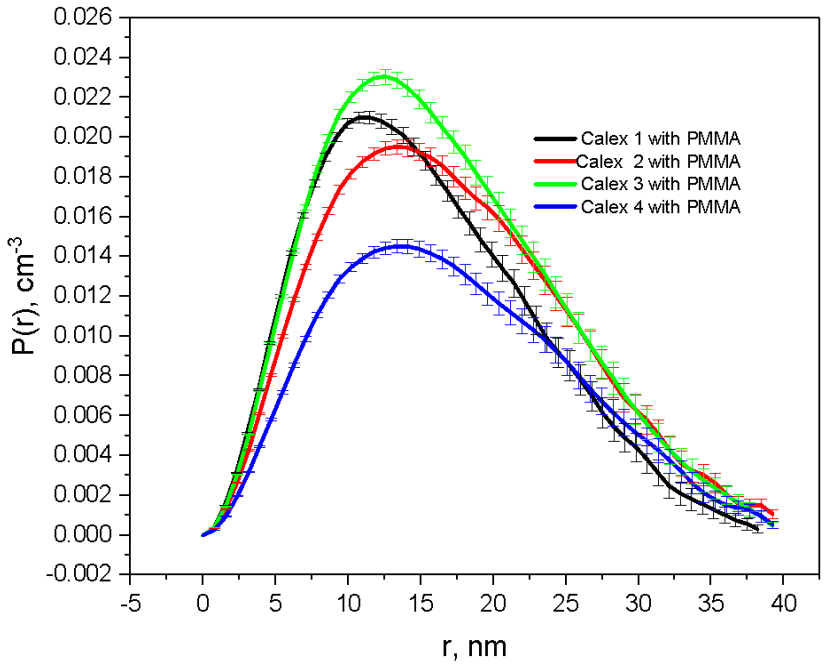

Fig. 8 - Pair distribution function for complexes calixarene C_1, C_2, C_3 and C_4

Additionally, atomic-force microscopy was used for size distribution of calixarene complexes C_1, C_2, C_3 and C_4. The corresponding results summarized in Table 3. Percentage of particle surface of a given fractions in relation to their total surface is calculated by the following expression [5]:

$$\Delta Q_{si} = \frac{s_i}{\sum s_i} \cdot 100 = \frac{n_i d_i^2}{\sum_i n_i d_i^2} \cdot 100 = f_{si} \cdot 100.$$

where s_i is the surface area of one particle with diameter d_i, n_i is the number of particles of fraction.

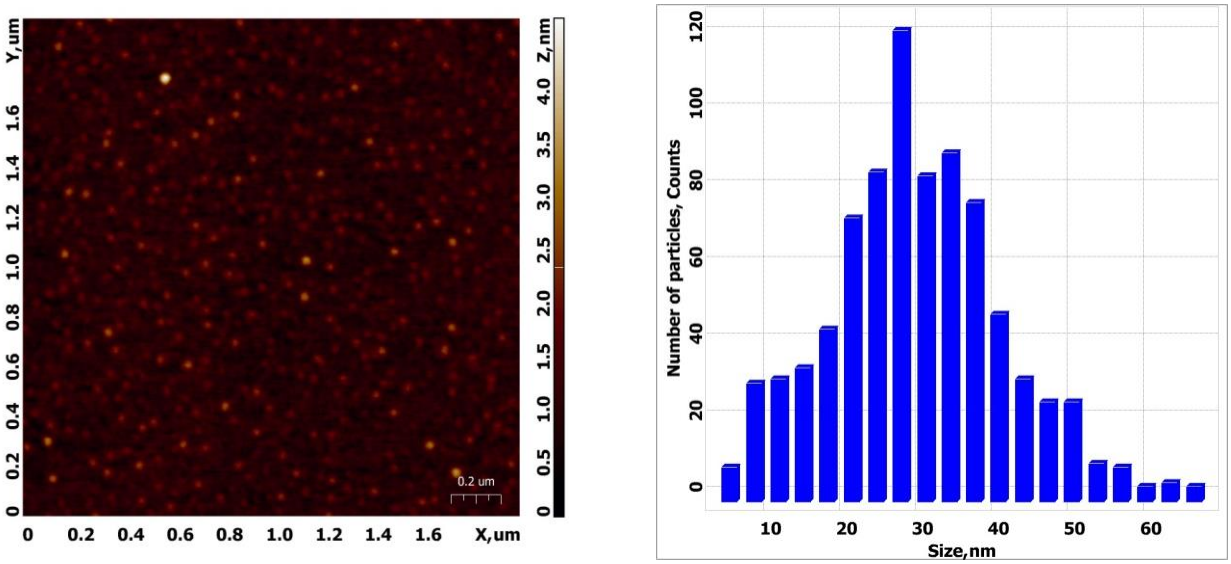

Fig. 9 - Right) sample C_1 image obtained with AFM; left) size distribution

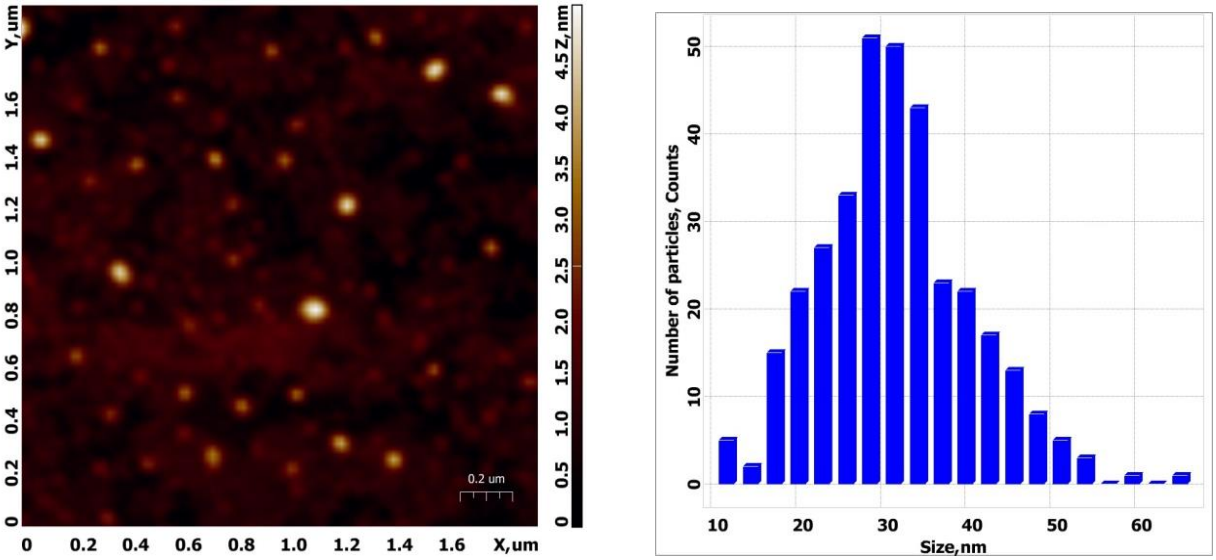

Fig. 10 - Right) sample C_2 image obtained with AFM; left) size distribution

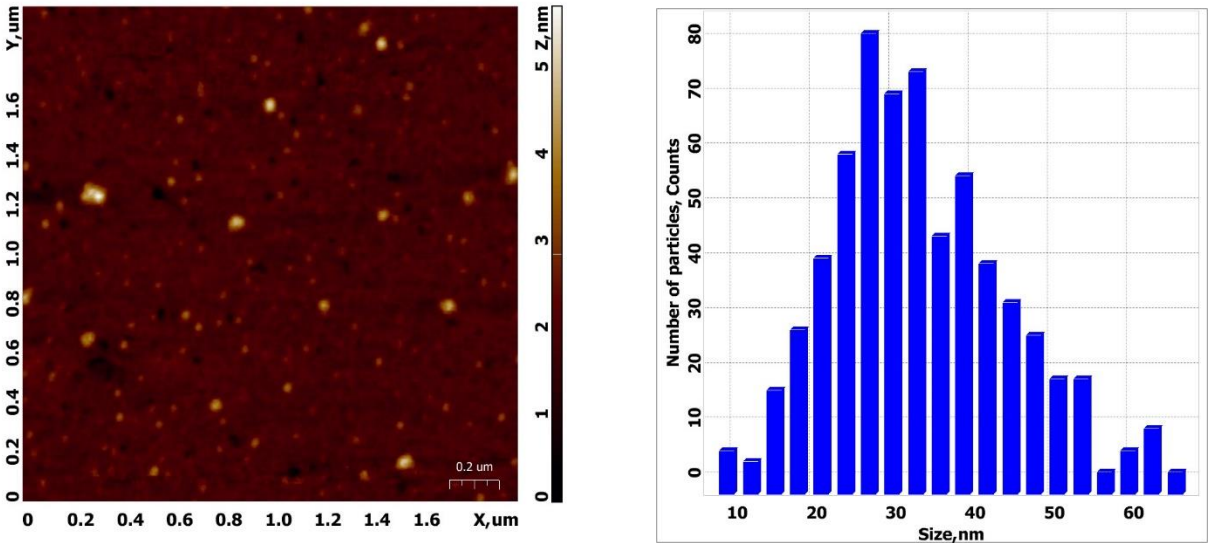

Fig. 11 - Right) sample C_3 image obtained with AFM; left) size distribution

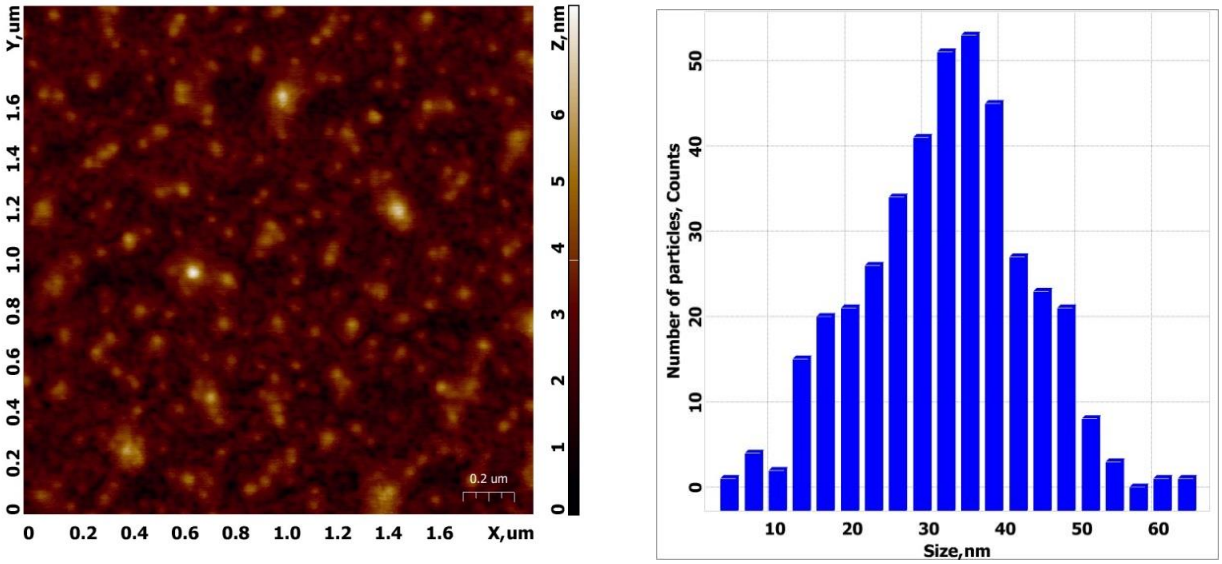

Fig. 12 - Right) sample C_4 image obtained with AFM; left) size distribution

Results and discussion.

An analysis of the parameters obtained from the processing of SANS curves using the generalized Guinier–Porod model shows that IPCs formed by calixarenes from two groups tend to be divided into two groups according to their structure (Table 3). The first group includes IPCs formed by C_1 and C_2 calixarenes with oxazoline arms in the upper rim of the calixarene basket; to the second group - calixarenes C_3 and C_4 with rays in the lower rim. IPCs formed by calixarenes C_1 and C_3, which have ethyl groups (Et) as substituents R in oxazaline fragments, have a larger size in each group: their gyration radius R_g reaches 46–48 Å. The radius of gyration R_g for IPCs formed by C_2 and C_4 calixarenes with isopropyl groups (i-Pr) as radicals in oxazoline arms is somewhat smaller, especially for C_2 + PMAA, the R_g value is only 37 Å. This result points to the hydrophobic role of the i-Pr groups

in the oxazoline fragments of C2 and C4 calixarenes. This leads to a more compact structure of their IPC.

Closest to cylindrical structures C_1 + PMAA with dimension parameter 3 – s equal to about 1,7. The closest to oblate plates is the C_2 + PMAA complex, in which the 3 – s dimension is 1.3. IPC from group **II**, in which oxazoline beams are attached to the lower rim, and in the upper rim there are also i-Pr groups that increase the hydrophobicity of the "basket" (see Fig. 1 **II**), in their structure they occupy an intermediate position between lamellas and cylinders at 3 – s between 1,5–1,6. Such a value may indicate a prolate ellipsoid of revolution that has a long axis of rotation and a smaller diameter.

	C_1	C_2	C_3	C_4
D_{SANS} from P(r) SASView, nm	31 (Rg=12nm)	34 (Rg=13nm)	34 (Rg=13nm)	34 (Rg=13nm)
D_{SANS} from P(r) Primusqt, nm	34.3 (Rg=13.2nm)	36.8 (Rg=14.1nm)	33.4 (Rg=12.8nm)	34.8 (Rg=13.4nm)
D_{AFM}, nm	31.8 (11)	33.0 (8)	35.5 (11)	34.8 (11)

Table 3 - Size of calixarene-PMMA complexes

For reconstruction of the calixarene complexes C_1, C_2, C_3 and C_4 RasMol software was used.

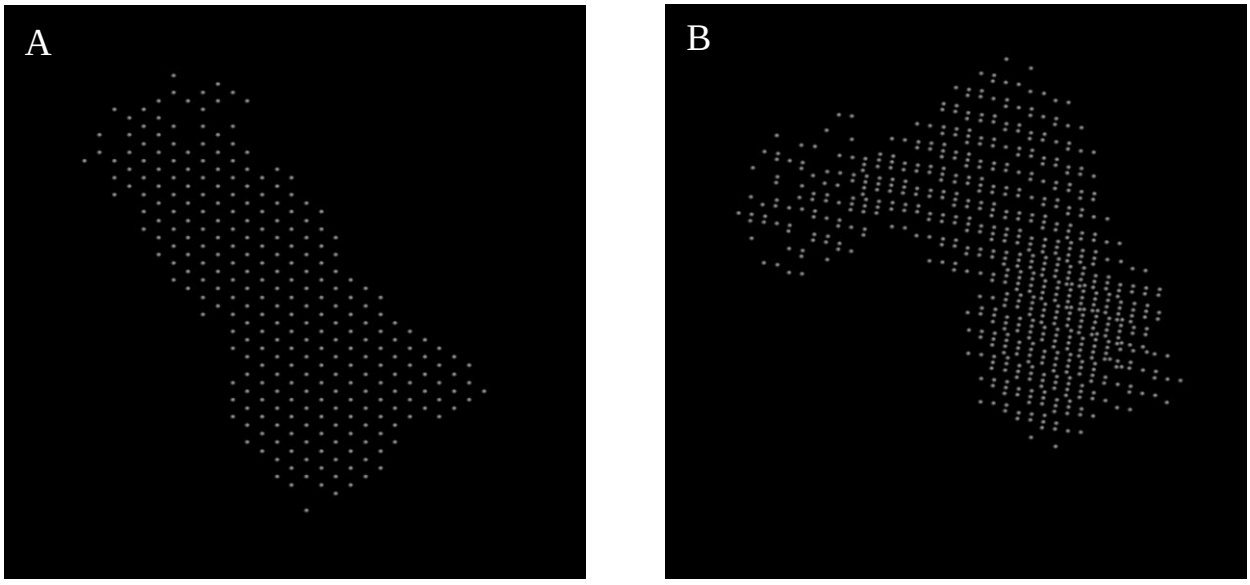

Fig. 13 - A) 2D; B) 3D visualization of the calikarene complex C_1

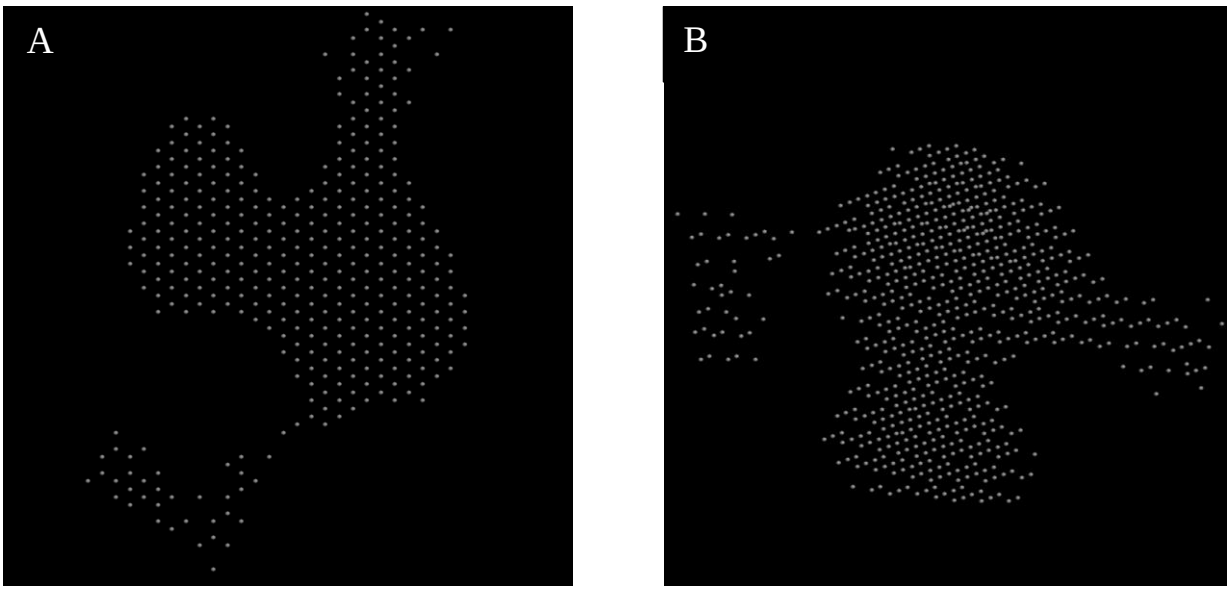

Fig. 14 - A) 2D; B) 3D visualization of the calikarene complex C_2

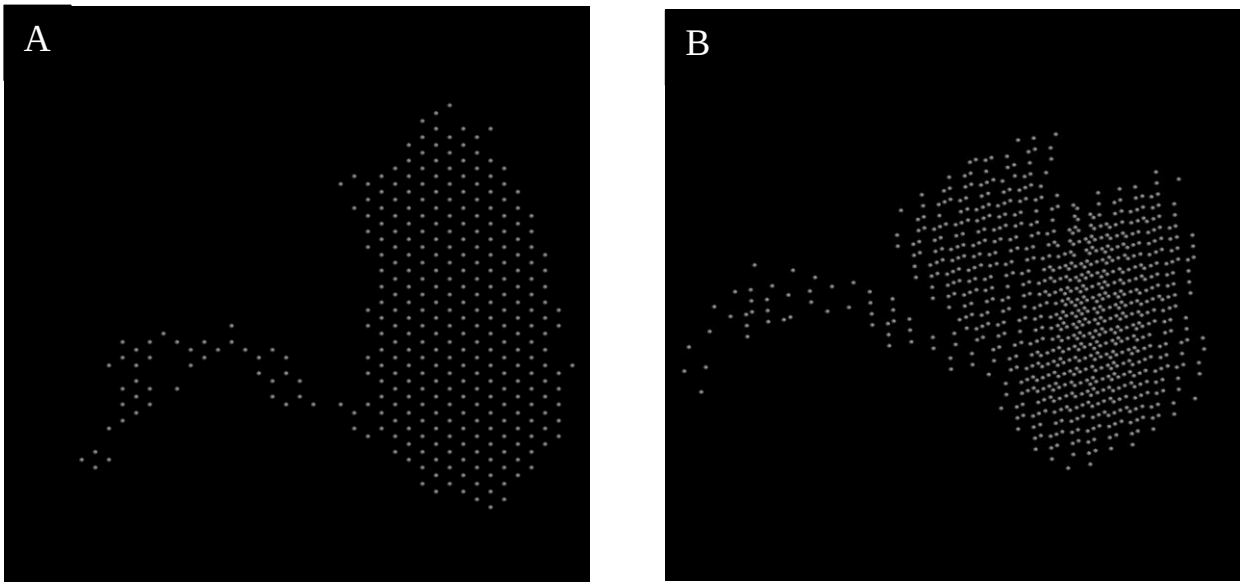

Fig. 15 - A) 2D; B) 3D visualization of the calikarene complex C_3

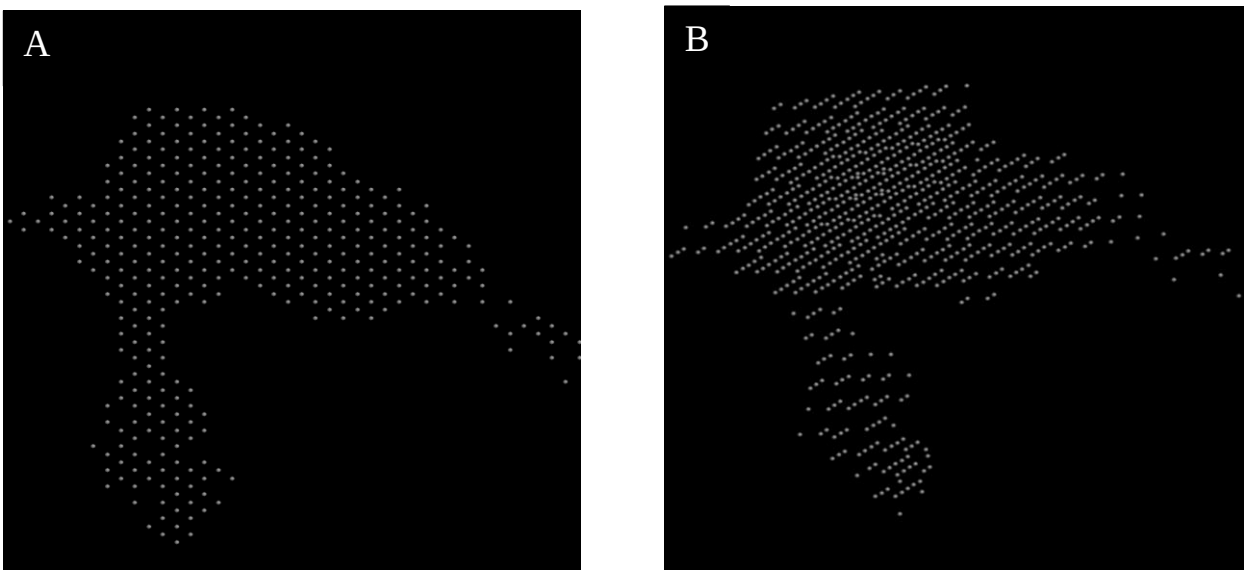

Fig. 16 - A) 2D; B) 3D visualization of the calikarene complex C_4

Conclusions

During the summer student practice under the START program at JINR, the methods of small-angle neutron scattering and atomic force microscopy were mastered. These methods were used to study the structure of new calixarene complexes containing eight-arm poly-2-alkyl-2-oxazoline arms with polymethacrylic acid. 4 systems of calixarenes differing in the monomer in their chain were investigated (Table 1). Specials skills for processing SANS curves by SasView and Primus softwares were obtained at JINR, too (Table 2). It was found that the structure of IPA complexes from group **I** C_1 + PMAA is close to cylindrical s = 1.3, while C_2 + PMAA is close to flattened plates s = 1.7. IPAs from group **II** occupy an intermediate position between lamellae and cylinders with s between 1.4–1.5. Also, based on the pair correlation function, the radius of gyration and the size of the C_1-C_4 complexes were determined (Table 3). Based on the obtained SANS curves, 2D and 3D visualization was carried out in the RasMol software. The particle size distribution obtained using AFM in the Nova software is in good agreement with the previously described results.

Fig. 17

Acknowledgment

I express my gratitude to the JINR Educational and Scientific Center for the opportunity to participate in the START program, for the lectures and tours of the Institute's laboratories. The skills and knowledge acquired at JINR are indispensable for my further scientific and technical activities.

I express my special gratitude to the scientific adviser Gorshkova Yu.E. for mentoring throughout the whole practice and help in mastering the material.

References

[1] D. I. Svergun, L. A. Feigin. Small-angle scattering. (http://www.femto.com.ua/articles/part_1/2147.html).

[2] Thomas M. Weiss Stanford University. Introduction to Small-Angle X-ray Scattering.

[3] Yuri Lyubchenko. Preparation of DNA and nucleoprotein samples for AFM imaging. (https://www.ncbi.nlm.nih.gov/pmc/articles/PMC2997872/).

[4] A. A. Lezov, A. S. Gubarev, A. N. Podsevalnikova. Temperature-responsive star-shaped poly(2-ethyl-2-oxazoline) and poly(2-isopropyl-2-oxazoline) with central thiacalixarene fragments: structure and properties in solutions.

[5] N. N. Gavrilova, V. V. Nazarov, O. V. Yarovaya. Microscopic methods for determining particles of dispersed materials. (https://www.muctr.ru/upload/iblock/637/6375684f7634dcfa06713798a00fd5b8.pdf).